Forward Modeling of a High Resolution X-ray Imaging Crystal Spectrometer for the Wendelstein 7-X Stellarator

A. Langenberg[1], H. Thomsen[1], R. Burhenn[1], O. Marchuk[2], J. Svensson[1], T.S. Pedersen[1], R.C. Wolf [1]

[1]*Max-Planck-Institut für Plasmaphysik, 17491 Greifswald, Germany*
[2] *Forschungszentrum Jülich GmbH, Institut für Energie- und Klimaforschung – Plasmaphysik, 52425 Jülich, Germany*

Introduction

For the measurement of radial ion temperature T_i and poloidal flow velocity profiles v_Φ at the Wendelstein 7-X (W7-X) stellarator, the installation of two high resolution X-ray imaging spectrometer systems of the Johann-type is under preparation [1-3]. Wavelength selection by Bragg-reflection (λ = 4 Å) is achieved with a spherically bent crystal [3], providing a radial profile of the He- or H-like spectrum of selected (mainly Argon due to a broad radial range of existence in the bulk plasma) impurities.

This paper presents a full forward modeling of the spatial and energy resolved intensity pattern on a 2D CCD detector of the High Resolution X-ray Imaging Spectrometer system HR-XIS [1] using the Minerva Bayesian analysis framework [4]. This framework provides an elegant way of calculating radial profiles of plasma parameters from line-integrated measurements.

1. Bayesian Modeling of the Spectrometer System

Bayesian Analysis is a standard method for the inversion of line integrated measurements in plasma physics and is widely used for several plasma diagnostics [4-8].

In this approach, predicted data $\boldsymbol{D^*}$, depending on a set of free parameters $\boldsymbol{N}$ (like ion and electron temperatures T_i and T_e) through a physics model $f\ (\boldsymbol{D^*} = f_f\ (\boldsymbol{N}))$, are expressed in terms of a *Probability Density Function (PDF),* considering the measurement uncertainties. The *likelihood distribution* $P(\boldsymbol{D}|\boldsymbol{N})$ generally denotes the probability of observed data for given parameters $\boldsymbol{N}$.

Applied to an imaging spectrometer, the likelihood of the observed counts for all pixels of a CCD detector is

$$P(\{D_p\}|N) = \prod_{p=0}^{Npix-1} \frac{1}{\sqrt{2\pi}\sigma_p} \exp\left(-\frac{(D^*_p - D_p)^2}{2\sigma_p{}^2}\right)$$

A normal distribution of photon statistics with a standard deviation σ_p is assumed. The predicted and observed numbers of counts are D^*_p and D_p for each pixel.

The solution to the inversion problem is an estimate of the free parameters $\boldsymbol{N}$ in this formulation. Bayes theorem is utilized for the calculation of the so called *posterior* distribution:

$$P(\boldsymbol{N}|\boldsymbol{D}) = P(\boldsymbol{D}|\boldsymbol{N})\, P(\boldsymbol{N}) / P(\boldsymbol{D})$$

yielding a probability distribution of the free parameters, given the measured data. The *prior* distribution $P(\boldsymbol{N})$ reflects any knowledge on the model parameters before the measurement took place, $P(\boldsymbol{D})$ is a normalization constant.

We assume, that the impurity radiation follows the coronal limit. The model parameters $\boldsymbol{N}$ denote the radial profiles of ion and electron temperatures $T_i(\psi_n)$ and $T_e(\psi_n)$, the electron density $n_e(\psi_n)$, Hydrogen-, Helium-, and Lithium-like impurity densities $n_Z^{H/He/Li}(\psi_n)$, and poloidal plasma rotation $v_\Phi(\psi_n)$. Here ψ_n denotes the normalized magnetic flux.

2. Forward Simulation

The dependencies between model parameters and predicted data are completely defined within a graphical model inside the Minerva Bayesian analysis framework. A simplified scheme for the forward model is shown in Fig.1:

Plasma parameters are parameterized as 1D functions of normalized flux $\boldsymbol{N}(\psi_n)$ and expressed as 3D functions $\boldsymbol{N}(x,y,z)$, using a plasma model $\psi(x,y,z)$ derived from theory-based W7-X plasma configurations. The spectral emission of He-like Ar impurities is calculated in the coronal limit [9] and evaluated along line-of-sight integrals considering the foreseen installation geometry of the spectrometer, simulating a 2D energy and spatial resolved intensity pattern $\boldsymbol{D}(E,\psi_n)$ on the detector.

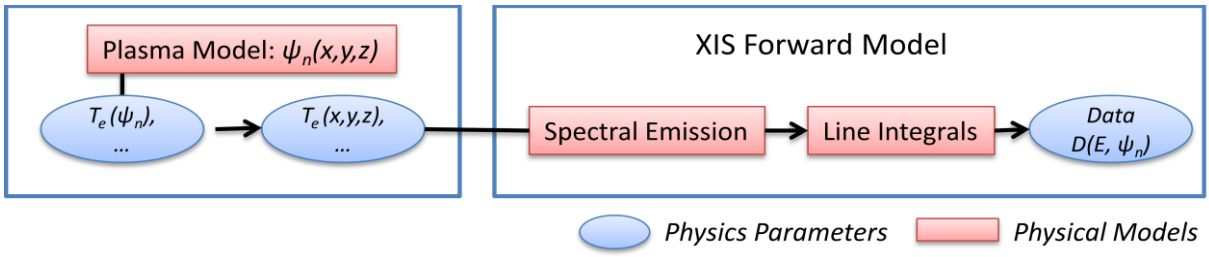

Fig.1: Simplified scheme for the forward model of an X-ray imaging spectrometer in the Minerva Bayesian analysis framework.

The data ***D*** for the 6 CCD detectors, each containing 1024 x 256 pixels (see Fig.2c), are calculated within the XIS forward model with a theoretical set of temperature and density profiles (cf. Fig 2a).

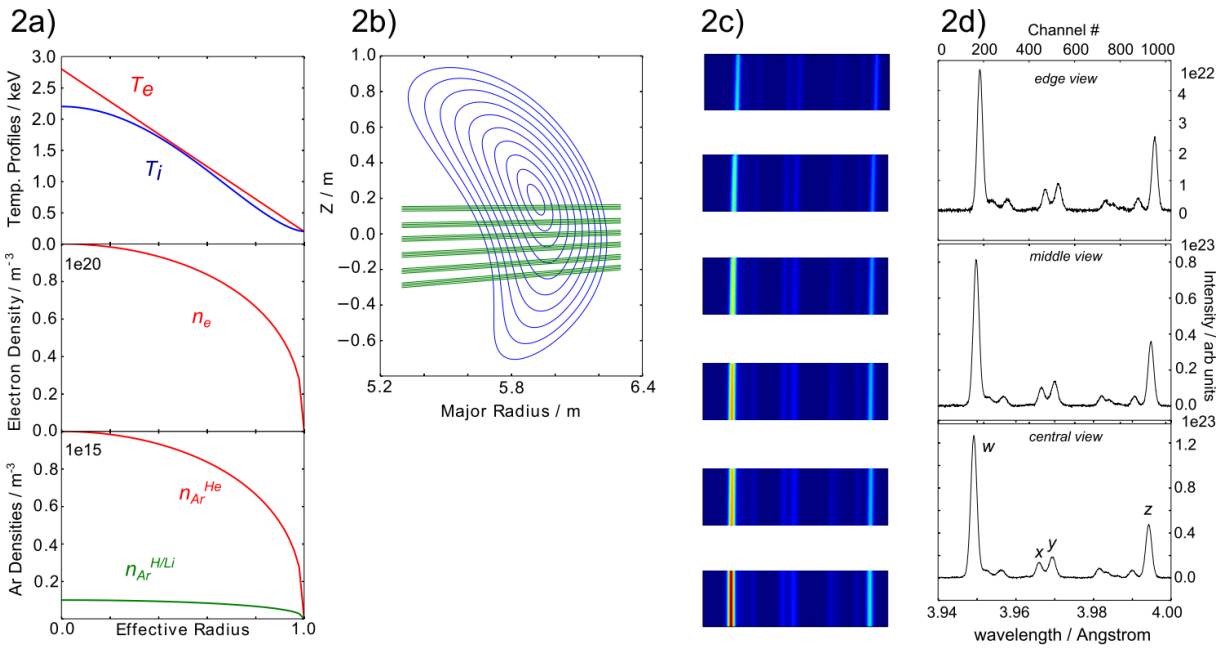

Fig.2: Forward simulated X-ray imaging spectrometer: 2a) Assumed temperature and density profiles of the free model parameters. 2b) The spectrometer's lines of sight with corresponding flux surfaces. 2c) Resulting 2D intensity pattern at the position of the CCD detector. Energy dispersion shows up along the horizontal axis, spatial resolution along the vertical axis. 2d) Line integrated spectra along central, middle and edge lines of sight.

The resulting 2D intensity pattern at the position of the CCD detector is shown in Fig.2c. Due to the rotational symmetry of Bragg diffraction, the focal lines on the detector are curved. To illustrate the changes in the spectra, moving from the plasma center towards the plasma edge, line integrated spectra along a single central, middle and edge line of sight are depicted in Fig.2d. The radial outward decreasing ion temperature results in narrower line widths towards the edge, while the decreasing electron temperature changes the line ratios and reduces the overall intensity of spectral lines (Fig.2d). Within the simulation, a statistical noise corresponding to a signal to noise ratio of 200 at the central line-of-sight has been added to the data. In measured spectra taken at TEXTOR, an inversion of intensity ratios between the w and z lines towards the plasma edge can be observed [10], induced by charge exchange and transport processes that have not been taken into account in this forward simulation approach.

3. Inversion of Simulated Data

In the following, the simulated data are taken as observed data, being the basis for the inversion process, exemplarily shown for the determination of the electron temperature profile. For the inversion, the total amount of 1024 x 6 x 256 forward simulated pixels has

been binned to 100 x 12 pixels according to an energy interval of 100 pixels between 3.94-3.96 Å and 12 lines of sight distributed evenly across the view field of the spectrometer.

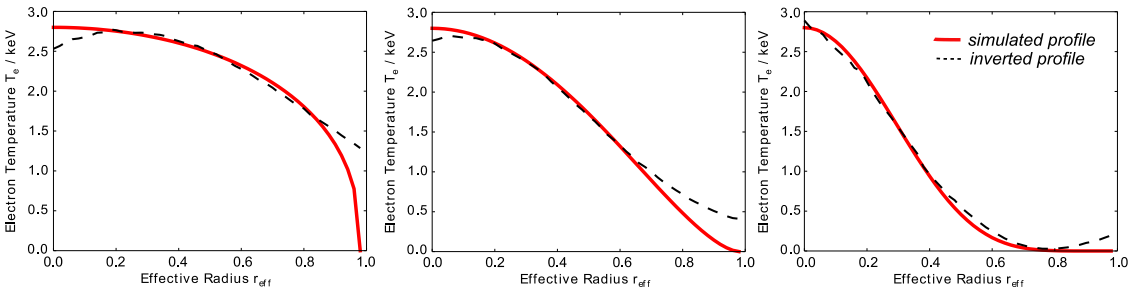

Fig.3: Simulated (solid red lines) and inverted electron temperature profiles (dashed black lines) inferred from forward simulated line integrated observations of an imaging spectrometer.

Non-parametric Gaussian processes have been used as model for the electron temperature profiles [6]. Starting from a constant temperature profile of T_e = 1keV, the profile with the highest posterior probability density – the *Maximum posterior* (MAP) has been derived within 20 iterations.

Figure 3 presents the inverted temperature profiles (dashed black) for several simulated profiles (solid red). Small deviations between assumed and inverted profiles at the plasma center and towards the edge region originate from the limited view field of the spectrometer, covering about ¼ of the whole plasma cross section, see Fig. 2b).

The model can be extended in order to deduce all model parameters in the inversion process and give estimations on the uncertainties of inverted profiles.

Acknowledgment

This project has received funding from the Euratom research and training programme 2014-2018.

[1] H. Thomsen, R. Burhenn, J. Assmann et al. 41th EPS Conference on Plasma Phys. Berlin (2014)

[2] N.A. Pablant, M. Bitter, R. Burhenn et al. 41th EPS Conference on Plasma Phys. Berlin (2014)

[3] G. Bertschinger, W. Biel, H. Jaegers et al. Review of Scientific Instruments 75 (2004)

[4] J. Svensson, A. Werner, IEEE International Symposium on Intelligent Signal Processing, (2007)

[5] O. Ford, PhD thesis, University of London, Imperial College London (2010)

[6] J. Svensson, A. Werner, Plasma Phys. Control. Fusion 50 (2008)

[7] M. Krychoviak, R. König, T. Klinger et al. Journal of Appl. Phys. 96 (2004)

[8] R. Fischer, A. Dinklage, and E. Pasch, Plasma Phys. Control. Fusion 45 (2003)

[9] O. Marchuk, PhD thesis, Forschungszentrum Jülich GmbH, Jülich (2004)

[10] T. Schlummer, PhD thesis, Forschungszentrum Jülich GmbH, Jülich (2014)